

Masaaki Mishima,^a Mustanir,^a Irina Eventova^b and Zvi Rappoport^{*b}
^a Institute for Fundamental Research of Organic Chemistry, Kyushu University, Hakozaki, Fukuoka 812-8521, Japan

^b Department of Organic Chemistry, The Hebrew University, Jerusalem 91904, Israel

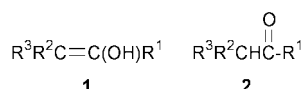
Received (in Cambridge, UK) 10th February 2000, Accepted 18th April 2000

Published on the Web 13th June 2000

The equilibrium constants for the ionization of nine stable simple enols and of eight ketones were determined by the ion cyclotron resonance (ICR) method in the gas phase. From these pK_{a} values, seven ketone–enol equilibrium constants K_{Enol} were calculated. The most acidic enol in the series $\text{Mes}_2\text{C}=\text{C}(\text{OH})\text{R}$ (**3**) is when $\text{R} = p\text{-CF}_3\text{C}_6\text{H}_4$ ($\Delta G_{\text{acid}}^\circ = 323.4 \text{ kcal mol}^{-1}$) and the least acidic one is when $\text{R} = t\text{-Bu}$ ($\Delta G_{\text{acid}}^\circ = 334.7 \text{ kcal mol}^{-1}$). There is a good correlation between the $\Delta G_{\text{acid}}^\circ$ values for the ketones and the enols. For 4 α -aryl-substituted enols ($\text{R} = \text{Ar}$) and their keto isomers, there is a rough correlation with Hammett's σ values. The $\Delta G_{\text{acid}}^\circ$'s for the enols where $\text{R} = \text{Ar}$ correlate linearly with their $\Delta G_{\text{acid}}^\circ$'s in hexane, but other enols deviate from the relationship. The pK_{a} 's and pK_{Enol} values were calculated by RHF/3-21G* and some values were calculated by B3LYP/3-21+G*. The observed $\Delta G_{\text{acid}}^\circ$'s for the enols give an approximately linear correlation with the calculated $\Delta E_{\text{acid}}^\circ$ values. However, the $\Delta G_{\text{eq}}^\circ$ values for the keto–enol equilibrium in the gas phase or in hexane do not correlate linearly with ΔE_{eq} for all the enols. The calculated Ar–C=C dihedral angles in the enols **3** change only slightly to modestly on ionization, presumably due to a relatively rigid geometry caused by steric hindrance. The substituent effects on the acidities and the K_{Enol} values are discussed.

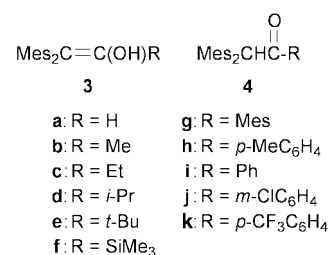
Introduction

In spite of the short life of most simple enols **1** of aldehydes

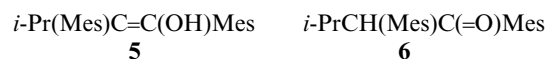


and ketones **2**,¹ research in the last 20 years has enabled the determination of many of the $\mathbf{2}=\mathbf{1}$ equilibrium constants K_{Enol} ($pK_{\text{Enol}} = -\log K_{\text{Enol}}$)² and the acidity constants pK_{a}^{E} of these species in water.³ The acidity constants pK_{a}^{K} of the carbonyl tautomers are usually also known, and the three equilibrium constants are connected by the relationship $pK_{\text{Enol}} = pK_{\text{a}}^{\text{K}} - pK_{\text{a}}^{\text{E}}$.

We have studied in recent years the chemistry of stable simple enols ("simple enols" were defined by Hart^{4a} as enols that contain no stabilising functionality such as C=O, NO₂, CN, etc.), where R² and R³ are bulky aromatic groups, mostly mesityls (Mes) and R¹ is an aliphatic or aromatic substituent.^{4b,c} The pK_{Enol} values for the 1-alkyl and 1-H keto–enol systems **3(a–e)**–**4(a–e)**⁵ and for several 1-aryl derivatives such as **3(g–k)**–**4(g–k)** (and a few others)^{6,7} were determined in hexane. A minimum value was estimated for the 1-SiMe₃ system **3f**–**4f**.⁸ In the aliphatic series **3(a–e)**–**4(a–e)** the pK_{Enol} values increase linearly with the increased steric parameter of the α -alkyl (H) group,⁵ whereas in the aromatic series **3(h–k)**–**4(h–k)** and the *p*-PhO, *p*-MeO, *m,m'*-Br₂ derivatives) pK_{Enol} is linear with respect to σ^+ with $\rho^+ = 0.65$.⁷ The pK_{a}^{E} values for eight of these enols in DMSO (17.8–19.9) were recently determined,⁹ and the effect of substituents on them was discussed. Four values (29–33) were previously determined in acetonitrile.¹⁰ However, the corresponding pK_{a}^{K} values, and hence the K_{Enol} values, in these solvents are unavailable.



The isomeric 1,2-dimesityl-2-alkylethenols and 1,2-dimesityl-2-alkylethanones of **3(b–d)**–**4(b–d)** were also investigated.¹¹ However, the pK_{Enol} values could not be determined due to a slow isomerization of the enols, especially enol **5** and to the lack of isomerization of the ketones, e.g., **6**. The pK_{Enol} values are likely to be ≥ 2 .



In the present work we determined, using the ion cyclotron resonance (ICR) method, eight pK_{a}^{K} , and nine pK_{a}^{E} values which gave the pK_{Enol} values for seven keto–enol pairs. This enables comparison with the solution data mentioned above, especially with K_{Enol} values in hexane, as well as several correlations with substituent parameters and the equilibrium data for related systems. Some MO calculations were also conducted on these systems in order to compare the experimental with the calculated values and to learn about the changes taking place on ionization. To the best of our knowledge these are the first pK_{Enol} values measured in the gas phase for systems in which the simple enols were introduced directly into the mass spectrometer rather than generated in the gas phase.¹²

Results and discussion

Measured pK_{a}^{E} and pK_{a}^{K} values

Fig. 1 gives the free energy changes (ΔG°) for the respective

† Optimised energies, and calculated bond lengths and charge distributions are available as supplementary data. For direct electronic access see <http://www.rsc.org/suppdata/p2/b0/b001155j>

Table 1 Observed acidities (kcal mol⁻¹) of Mes₂C=C(OH)R (**3**) and Mes₂CHC(=O)R (**4**) in the gas phase

R	$\Delta G_{\text{acid}}^{\circ}(\mathbf{3})$	$\Delta G_{\text{acid}}^{\circ}(\mathbf{4})$	$\Delta G_{\text{eq}}^{\circ}((\mathbf{4})-(\mathbf{3}))$	pK_{Enol}	$\Delta G_{\text{eq}}^{\circ}(\text{hexane})^a$	$pK_{\text{Enol}}(\text{hexane})$
H	332.8					
Me		335.3				
<i>t</i> -Bu	334.7	336.5	1.8	1.33	3.6	2.66
Ph	328.7	329.3	0.6	0.44	-0.01	-0.007
Mes	330.9	330.6	-0.3	-0.22	-3.1	-2.3
<i>p</i> -CF ₃ C ₆ H ₄	323.4	322.6	-0.8	-0.59	-0.76	-0.56
<i>m</i> -ClC ₆ H ₄	327.0	326.8	-0.2	-0.15	-0.56	-0.41
<i>p</i> -MeC ₆ H ₄	330.2	331.2	1.0	0.74	0.23	0.17
SiMe ₃		333.9				
Mes(<i>i</i> -Pr),Mes	337.2 ^b	339.5 ^c	2.3	1.70	>2.7	>2.0

^a Ref. 5–8. ^b For **5**. ^c For **6**.

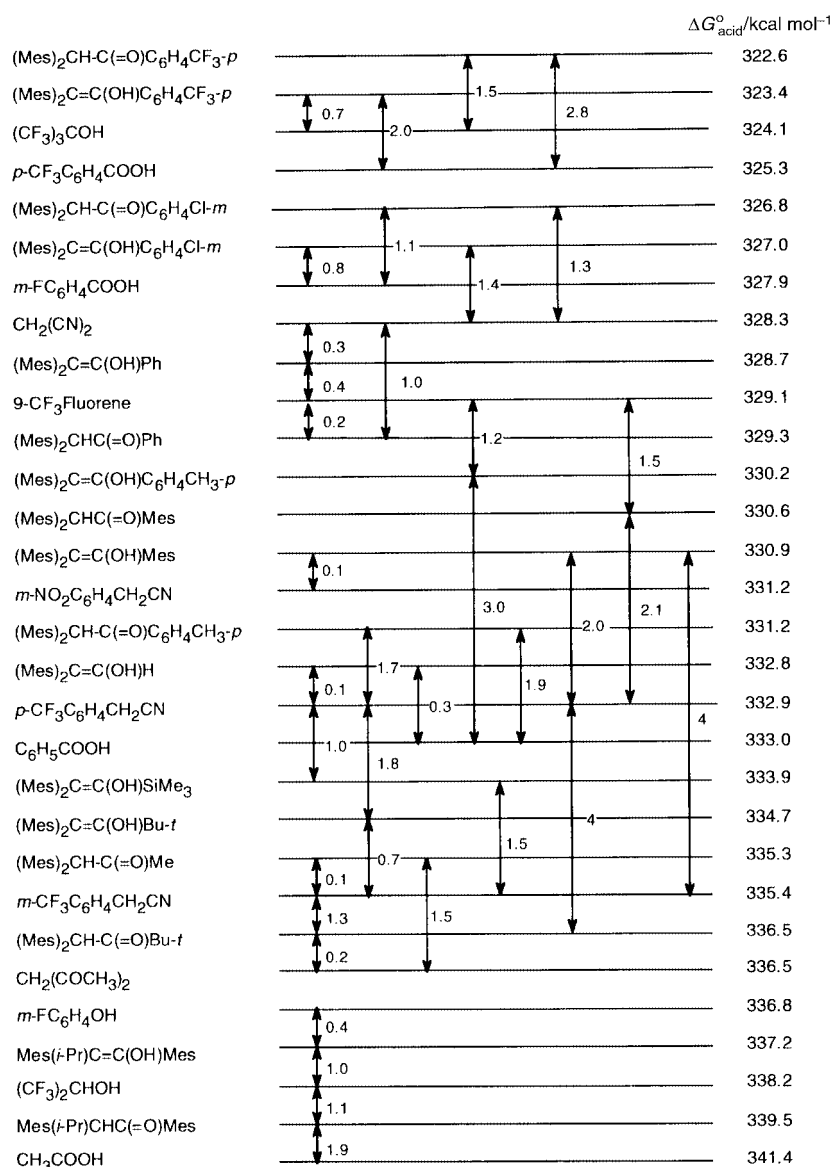
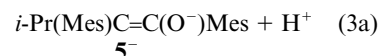
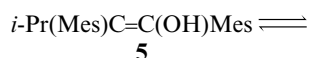
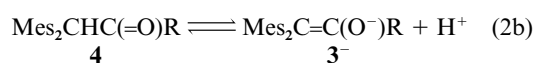


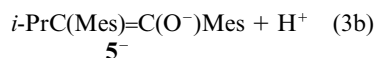
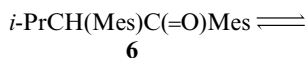
Fig. 1 Free energy changes for respective proton-transfer equilibria and $\Delta G_{\text{acid}}^{\circ}$ values (kcal mol⁻¹).

proton transfer equilibria between the enols **3**, the ketones **4** and the reference acids with known acidities. The acidity ($\Delta G_{\text{acid}}^{\circ}$) value of an acid AH is defined by the free energy change of the following reaction (eqn. (1)). Table 1 gives the $\Delta G_{\text{acid}}^{\circ}$ values for



the acid ionizations of both the enols **3a,e,f,g-k**, **5** and the ketones **4b,e,g-k** and **6** in the gas phase (eqns. (2a), (2b), (3a) and (3b))





where $\mathbf{3}^-$ and $\mathbf{5}^-$ are the anions derived from $\mathbf{3}$ and $\mathbf{5}$, respectively), the derived $\Delta\Delta G_{\text{acid}}^\circ$ values (where $\Delta\Delta G_{\text{acid}}^\circ = \Delta\Delta G_{\text{eq}}^\circ$) and the $\text{p}K_{\text{Enol}}$ values. The $\text{p}K_{\text{Enol}}$ values in hexane^{5-8,11} are given for comparison.

The possibility that a ketone–enol isomerization takes place during the experiment is excluded by the reproducibility of the $\Delta G_{\text{acid}}^\circ$ values even when a new experiment with a previously heated sample is compared with that for a fresh sample and by the different $\Delta G_{\text{acid}}^\circ$ values for the enol and the ketone for each pair of isomers. The most acidic enol of those studied is $\mathbf{3k}$ with the 1-*p*-F₃CC₆H₄ substituent ($\Delta G_{\text{acid}}^\circ = 323.4 \text{ kcal mol}^{-1}$) and the least acidic enol measured is $\mathbf{5}$ ($\Delta G_{\text{acid}}^\circ = 337.2 \text{ kcal mol}^{-1}$). The least acidic enol in series $\mathbf{3}$ is $\mathbf{3e}$ ($\Delta G_{\text{acid}}^\circ = 334.7 \text{ kcal mol}^{-1}$), and the 11.3 kcal mol⁻¹ difference from $\mathbf{3k}$ is larger than the differences measured between the most acidic and least acidic enols studied in DMSO⁹ or MeCN¹⁰ solutions. The most acidic ketone measured is again the 1-*p*-F₃CC₆H₄ substituted ($\mathbf{4k}$) with $\Delta G_{\text{acid}}^\circ$ of 322.6 kcal mol⁻¹, and the least acidic in the $\mathbf{4}$ series is the 1-*t*-Bu ketone $\mathbf{4e}$ ($\Delta G_{\text{acid}}^\circ = 336.5 \text{ kcal mol}^{-1}$), the $\Delta\Delta G^\circ$ difference being 13.9 kcal mol⁻¹. Ketone $\mathbf{6}$ is formally less acidic than $\mathbf{4e}$, with $\Delta G_{\text{acid}}^\circ = 339.5 \text{ kcal mol}^{-1}$ but it is questionable (see below) whether the acidity measured is indeed the thermodynamic acidity.

Acidity and K_{Enol} correlations

There is an excellent correlation (eqn. (4)) between the seven

$$\Delta G_{\text{acid}}^\circ (\mathbf{3} \text{ or } \mathbf{5}) = 59.3 + 0.82 \Delta G_{\text{acid}}^\circ (\mathbf{4} \text{ or } \mathbf{6}) \quad n = 7 \quad R^2 = 0.992 \quad (4)$$

observed ΔG° values for the enols' $\Delta G_{\text{acid}}^\circ$ ($\mathbf{3}$ or $\mathbf{5}$) and for the corresponding ketones' $\Delta G_{\text{acid}}^\circ$ ($\mathbf{4}$ or $\mathbf{6}$), which include five aromatic α -substituents and the α -*t*-Bu group in the $\mathbf{3/4}$ series, and the $\mathbf{5/6}$ pair (Fig. 2). The substituent effects on the enols and the ketones are therefore parallel, but the slope of 0.82 indicates the somewhat higher sensitivity of the acidity to the substituents in the keto series. Since the two species generate the same anion, the linear correlation is equivalent to that between the energies of the neutral enols and ketones. The higher sensitivity to the substituent in the ketone series may be related to the initial higher polarization of the O–H of the enols compared with the C–H bond of the ketone. On the other hand, the conjugation of the C=O bond in the ketones is better than of the C=C bond in the enols.

For the four aromatic enols $\mathbf{3h-k}$ and for the four ketones $\mathbf{4h-k}$ approximate linear Hammett plots with σ (eqns. (5a) and (5b)) values which are better than those with σ^+ (where $R^2 =$

$$\Delta G_{\text{acid}}^\circ = -8.51\sigma + 328.9 \quad n = 4 \quad R^2 = 0.902 \quad (5a)$$

$$\Delta G_{\text{acid}}^\circ = -10.97\sigma + 329.5 \quad n = 4 \quad R^2 = 0.931 \quad (5b)$$

0.876 and 0.903, respectively), were observed. The negative slopes indicate that electron-attracting substituents increase the acidity of both the enols and the ketones, as expected.

The observed gas phase $\text{p}K_{\text{a}}$'s of enols $\mathbf{3}$ could be compared with the recently determined⁹ $\text{p}K_{\text{a}}$ values in DMSO. Data are available for R = H, Mes, Me₃Si, Ph and *t*-Bu. The order of $\text{p}K_{\text{a}}$ values in DMSO for R is H < Ph < Mes ~ Me₃Si < *t*-Bu, whereas the present gas phase data give the order Ph < Mes < H < SiMe₃ < *t*-Bu, *i.e.*, the three enols with α -H, α -*t*-Bu or α -SiMe₃ substituents are less acidic than the α -aryl-substituted ones. Their acidity varies with the α -R substituent in the order H(332.8) > SiMe₃(333.9) > *t*-Bu(334.7), which is equivalent to that found in DMSO as shown by the three point $\Delta G_{\text{acid}}^\circ$

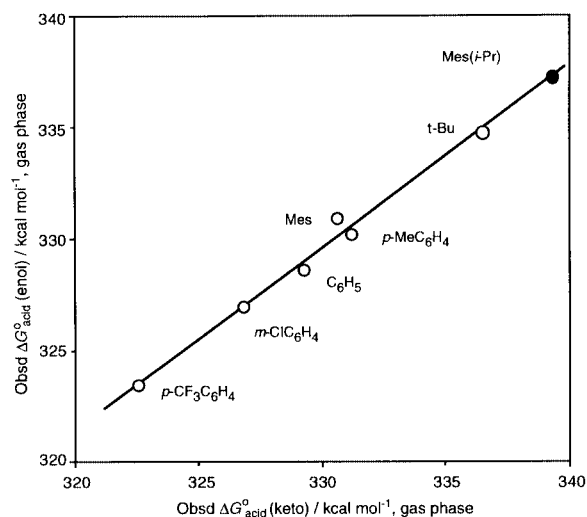


Fig. 2 Correlation of the observed $\Delta G_{\text{acid}}^\circ$ values for enols $\mathbf{3}$ vs. ketones $\mathbf{4}$. The black point is for the $\mathbf{5/6}$ pair.

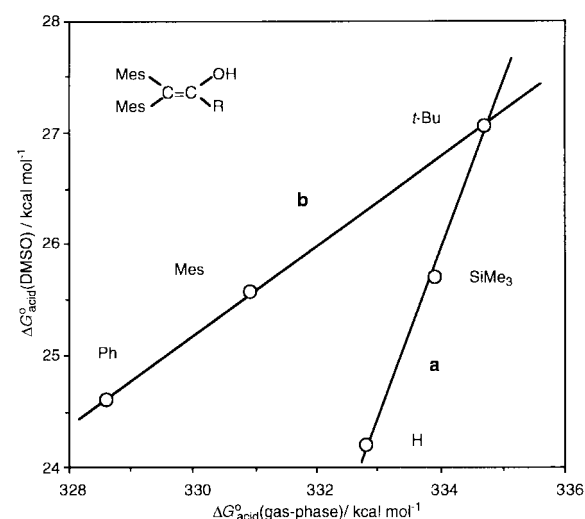


Fig. 3 Comparison of acidities of the enols in DMSO and in the gas phase. **a**: slope = 1.49 ($R^2 = 0.996$); **b**: slope = 0.41 ($R^2 = 0.999$).

(DMSO) vs. $\Delta G_{\text{acid}}^\circ$ (gas phase) correlation (Fig. 3a). Viewed in this way, the slope for the points for Ph and Mes (0.41) shows much lower sensitivity than for the other groups. However, viewed differently, there is a linear correlation of the Ph, Mes and *t*-Bu groups (Fig. 3b) with the points for H and SiMe₃ being outliers. The differences between the $\Delta G_{\text{acid}}^\circ$ values in the gas phase and in DMSO solution should reflect the differential solvation of the enol and its anionic species by DMSO. In DMSO the neutral enol is solvated by hydrogen bonding to DMSO as can be deduced by the rough correlation between $\log K_{\text{assoc}}$ ¹³ and $\text{p}K_{\text{a}}$ (DMSO) [K_{assoc} is the association constant of the enols with DMSO]. In addition, the charged species are solvated by the high relative permittivity solvent. The difference in $\Delta G_{\text{acid}}^\circ$ in the two media is enormous and it is reasonable to assume a higher response to the substituents in the gas phase than in DMSO, *i.e.*, a slope < 1 as in Fig. 3b. Indeed, for the related phenols the slope of the plot of $\Delta G_{\text{acid}}^\circ$ in the gas phase vs. that in DMSO is 2.88.¹⁴ In this case the α -H and α -SiMe₃ enols are less acidic in the gas phase (or more acidic in DMSO) than is predicted by Fig. 3a.

Since all four substituents (excluding H) are bulky and polarizable, and higher polarizability will increase the stabilization of $\mathbf{3}^-$ in the gas phase more than in DMSO, the deviation of enol $\mathbf{3a}$ with the small α -H substituent should not be surprising. Support for the importance of polarizability is obtained from the calculated charge distribution in $\mathbf{3}$, discussed below. In spite

of the higher electron donation of *t*-Bu compared with Me, the relative negative charge on R follows the order **3e** > **3b** > **3a**. The relative charge on the silicon of Me₃Si is positive, in contrast with the other groups (except H) and this may be the cause of the deviation from Fig. 3b.

In CH₃CN it has also been found that $pK_a^E(\mathbf{3e}) > pK_a^E(\mathbf{3a})$.¹⁰ The higher acidity of the α -H enol is consistent with the lower electron donation of H compared with *t*-Bu. The relative acidities of the α -*t*-Bu and α -SiMe₃ substituted enols were previously extensively discussed in relation to the pK_a 's in DMSO.⁹

The α -mesityl-substituted enol **3g** ($\Delta G_{\text{acid}}^\circ = 330.9$) is 2.2 kcal mol⁻¹ less acidic than the α -phenyl-substituted enol **3i** ($\Delta G_{\text{acid}}^\circ = 328.7$). This order is similar to that in DMSO where the $\Delta\Delta G_{\text{acid}}^\circ$ value is smaller, but is opposite to the value in CH₃CN. Electron donation by the three methyl groups is sufficient to explain the difference, although the slightly lower acidity of **3g** compared with that of the 1-*p*-tolyl-substituted enol **3h** may indicate that a small steric effect in the ionization of **3g** also plays a role.

The gas phase $\Delta G_{\text{acid}}^\circ$ value for the ionization of benzyl alcohol is 363.3 kcal mol⁻¹,¹⁵ and for phenol 342.3 kcal mol⁻¹,¹⁵ compared with 328.7 kcal mol⁻¹ for **3i**. Thus the substitution of the benzylic hydrogens in PhCH₂OH by a 2,2-dimesitylvinylidene unit increases the acidity by *ca.* 35 kcal mol⁻¹. This is an outcome of the electron-withdrawing effect of the sp²-hybridized carbon and apparently the ability of the β -mesityl groups to delocalize the negative charge in the enolate ion.

Comparison with phenol shows that phenol in DMSO has an almost identical pK_a value to that of **3a** and **3i** whereas in the gas phase it is 14 and 10 kcal mol⁻¹ more acidic. It is of interest to compare the gas phase acidities of the α -substituted *meta*- and *para*-substituted enols with those of the corresponding phenols.¹⁵ A plot of the gas phase $\Delta G_{\text{acid}}^\circ$ for the enols **3h–k** *vs.* those for the phenols gives an approximate linear correlation ($R^2 = 0.931$) with a slope of 0.46. The lower sensitivity in the enol series is expected since the OH group is one carbon removed from the aryl groups compared with the situation in the phenols and the slope of 0.46 is in the range expected for shielding of the =C moiety. Unfortunately, $\Delta G_{\text{acid}}^\circ$ data for substituted benzyl alcohols are not available for comparison. Interestingly, a similar plot of $\Delta G_{\text{acid}}^\circ$ values for the ketones **4h–k** *vs.* the phenols gives a better correlation with a slope of 0.59 ($R^2 = 0.955$). A similar shielding for the same reason was observed when comparing gas phase $\Delta G_{\text{acid}}^\circ$ values for ketones **4h–k** with the corresponding substituted toluenes.¹⁵ The slope of the correlation is 0.52 ($R^2 = 0.964$). The plot of $\Delta G_{\text{acid}}^\circ$ for the enols *vs.* the toluenes gives a slope of 0.40 ($R^2 = 0.944$).

Ketones **4** are significantly more acidic than simple aliphatic carbonyl compounds. The gas phase acidities for CH₃C(=O)R, where R = H, Me, *t*-Bu and Ph ($\Delta G_{\text{acid}}^\circ = 359.0, 361.9, 361.4$ and 354.4 kcal mol⁻¹, respectively)¹⁵ are *ca.* 25 kcal mol⁻¹ less acidic than our ketones. Obviously, negative charge resonance dispersal by the large polarizable β -mesityl groups is an important contributor to the high stability. The effects of the α -substituents are proportional in both series, $\Delta G_{\text{acid}}^\circ$ correlation of the three carbonyls *vs.* the ketones (**4**) gives a slope of 1.1 ($R^2 = 0.954$) and a much better plot *vs.* enols **3** gives a slope of 1.16 ($R^2 = 0.999$).

For the seven pairs of compounds where $\Delta G_{\text{acid}}^\circ$ values for both the ketone and the enol are known, the $\Delta G_{\text{eq}}^\circ = \Delta\Delta G^\circ$ (keto–enol) ($=\Delta G_{\text{acid}}^\circ$ (ketone) – $\Delta G_{\text{acid}}^\circ$ (enol)) values are given in Table 1, together with the derived pK_{Enol} values. These values qualitatively reflect the data in hexane, as shown by the $\Delta G_{\text{eq}}^\circ$ and pK_{Enol} values in Table 1.^{5–7} A plot of the $\Delta G_{\text{eq}}^\circ$ in hexane *vs.* $\Delta G_{\text{eq}}^\circ$ in the gas phase shows a very good correlation ($R^2 = 0.983$) for the four non-bulky α -aryl substituents with a slope of 0.57, with the mesityl and *t*-Bu points being outliers on both sides of the line (Fig. 4). The deviation of Mes reflects a polarizability effect of the bulkier aromatic ring, which is superimposed on the electronic effect reflected by the line for the other aryl-substituted systems. The slope which is less than

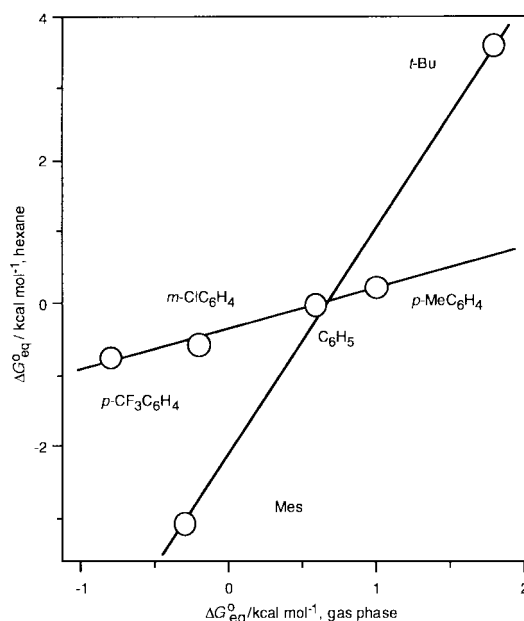


Fig. 4 A plot of $\Delta G_{\text{eq}}^\circ$ in hexane *vs.* $\Delta G_{\text{eq}}^\circ$ in the gas phase.

unity indicates a lower sensitivity to the substituents in hexane than in the gas phase.

The calculated $\Delta G_{\text{eq}}^\circ$ for the **5/6** pair is 2.3 kcal mol⁻¹ ($pK_{\text{Enol}} = 1.7$) which is consistent with the observed higher stability of **6** in hexane. However, the approach to equilibrium from the side of **6** is slow (*cf.* Experimental section) indicating that the pK_a value may be a measure of the kinetic rather than the thermodynamic acidity, and hence caution should be exercised if the derived K_{Enol} value is to be compared with the other K_{Enol} values measured here. In sterically crowded compounds proton transfer reactions in the gas phase are usually slow. The calculated optimized geometry of **6** indeed shows that approach to the acidic hydrogen is completely hindered by the *i*-Pr group compared with the other ketones (**4**) studied by us. It is noteworthy that likewise the catalyzed isomerization of **5** to **6** is very slow in solution even under severe conditions, and this was also ascribed to steric effects in approaching the reaction site.¹¹

Calculated pK_a and pK_{Enol} values

The availability of observed gas phase pK_a values encouraged calculations of these values which should be directly comparable with the experimental values. The geometries of nine enol–ketone pairs were optimized at the RHF/3-21G* level to give the energies of the enols, ketones and their free anions. Due to limited time, this low level calculation is the highest level of calculation for all the enols which is available to us. Since this method is unsuitable for calculations involving anions, four systems **3a–4a**, **3b–4b**, **3e–4e** and **3i–4i**, as well as their anions were calculated with the Hybrid Density Functional Theory with the B3LYP Functional using the 3-21+G* (and the 3-21G*) basis set. The energies of the various species are given in Table S1 in the electronic supplementary information. The ΔE_{acid} values for the ionization equilibria of the enols and the ketones (eqn. (1)) and for the keto–enol equilibria (ΔE_{eq}) are given in Table 2.

The RHF/3-21G* calculated ΔE_{acid} values differ significantly (by an average of *ca.* 34 kcal mol⁻¹) from the measured values for both the ketones and the enols. The B3LYP/3-21+G* values which involve diffuse p-type functions on all non-hydrogen atoms and hence are more suitable to describe the anions show smaller, but still significant deviations of 5.9–11.6 (average 9) kcal mol⁻¹ from the experimental values. Nevertheless, when the observed $\Delta G_{\text{acid}}^\circ$ values are plotted against the calculated RHF/3-21G* ΔE_{acid} values for seven ketones (excluding **6**) and the nine enols, an approximate, but far from perfect correlation

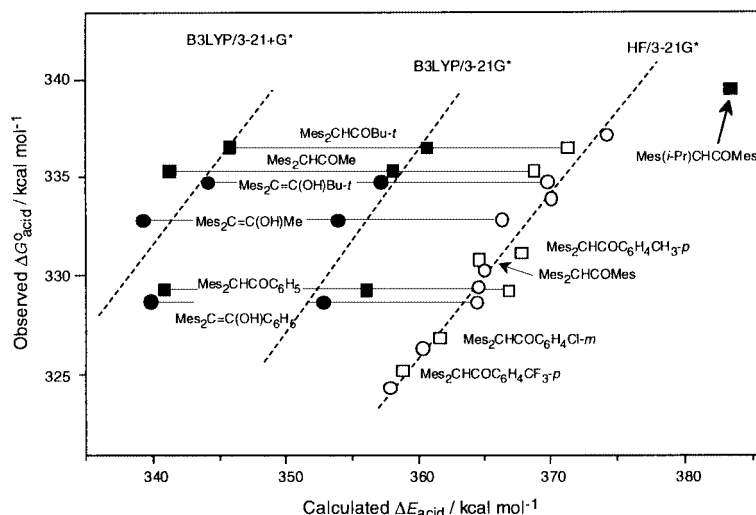


Fig. 5 Observed gas phase acidities of enols **3** and ketones **4** vs. the calculated ΔE_{acid} values at three calculation levels. Circles: enols. Squares: ketones. The point for ketone **6** was not used for obtaining the top correlation line.

Table 2 Calculated acidities (ΔE_{acid}) and keto–enol equilibria (ΔE_{eq}) of $\text{Mes}_2\text{C}=\text{C}(\text{OH})\text{R}$ and $\text{Mes}_2\text{CHC}(\text{=O})\text{R}$ at the RHF/3-21G* and B3LYP/3-21+G* levels

R	Level ^a	$\Delta E_{\text{acid}}(\text{enol})^b$	$\Delta E_{\text{acid}}(\text{ketone})^b$	ΔE_{eq}^c
H	A	366.30	362.57	-3.73
	B	339.27	335.20	-4.07
	C	354.85	348.92	-5.93
Me	A	369.84	368.72	-1.12
	B	342.23	341.22	-1.01
<i>t</i> -Bu	A	369.71	371.12	1.41
	B	344.14	345.75	1.61
Ph	A	364.52	366.83	2.31
	B	339.93	340.87	0.94
Mes	A	364.63	364.60	-0.03
<i>p</i> -CF ₃ C ₆ H ₄	A	357.91	358.85	0.94
<i>m</i> -ClC ₆ H ₄	A	360.29	361.69	1.40
<i>p</i> -MeC ₆ H ₄	A	365.11	367.72	-2.61
SiMe ₃	A	370.02	362.51	-7.51
Mes(<i>i</i> -Pr), Mes ^d	A	374.19	383.29	9.10

^a A: RHF/3-21G*; B: B3LYP/3-21+G*; C: RHF/3-21+G*. ^b Calculated acidities, in kcal mol⁻¹. ^c Calculated energy change of the keto–enol equilibrium, $E(\text{ketone}) - E(\text{enol})$, in kcal mol⁻¹. ^d For **5** and **6**.

was obtained (eqn. (6) and Fig. 5). Inclusion of **6** reduces R^2 to

$$\Delta G_{\text{acid}}^{\circ} = -3.6 + 0.91 \Delta E_{\text{acid}} \quad n = 16 \quad R^2 = 0.913 \quad (6)$$

0.860. The individual lines for the enols and the ketones (**6** excluded) gave better and nearly identical correlations (enols: slope = 0.83, $R^2 = 0.953$; ketones: slope = 1.06, $R^2 = 0.908$). On the other hand when the calculated ΔE_{acid} of the enols were plotted against those for the ketones, the four aryl-substituted systems (Mes excluded) gave a perfect correlation with $R^2 = 1.000$ but the points for aliphatic enols (α -H, Me, *t*-Bu, SiMe₃) and Mes were above the line. Plots of the calculated ΔE_{acid} vs. $\Delta G_{\text{acid}}^{\circ}$ values for **3a**, **3e**, **3i**, **4b**, **4e** and **4i** at B3LYP/3-21G* and B3LYP/3-21+G* show a similar trend. The slopes of all three correlations are similar, although the spread of the points was larger at the higher level methods (Fig. 5). This encourages a qualitative discussion of the RHF/3-21G* data.

Whereas the discrepancy between the calculations at the RHF/3-21G* and B3LYP/3-21+G* levels for the neutral ketones and enols is also large (Table 2), the differences in the ΔE_{eq} values are small. For α -H, α -Me and α -*t*-Bu the values differ by 0.1–0.3 kcal mol⁻¹ and for α -Ph by 1.4 kcal mol⁻¹. Hence, the $\Delta G_{\text{eq}}^{\circ}$ values (which are parallel to the $\text{p}K_{\text{Enol}}$ values) in hexane^{5,7,8} could be compared with the calculated RHF/

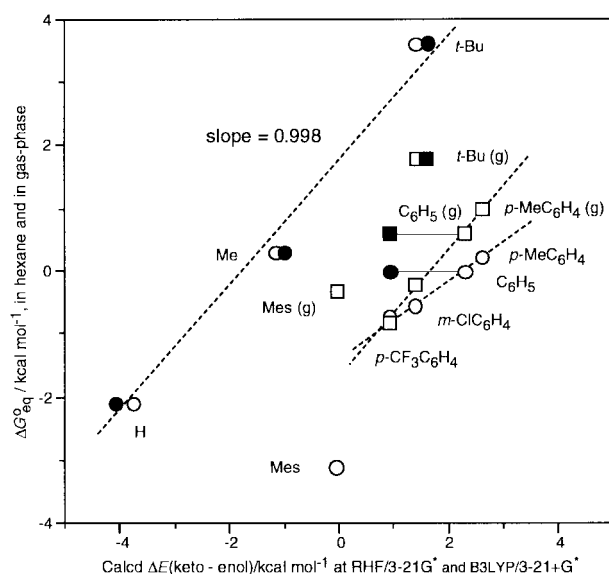


Fig. 6 $\Delta G_{\text{eq}}^{\circ}$ in hexane vs. the calculated RHF/3-21G* (○) and B3LYP/3-21+G* ΔE_{eq} values (●), and in the gas phase vs. the RHF/3-21G* (□) and B3LYP/3-21+G* (■) values.

3-21G* ΔE_{eq} values in the gas phase. Fig. 6 shows that for the four non-crowded aromatic substituents, the correlation is linear ($R^2 = 0.993$) with a small slope of 0.59, whereas the point for Mes is below the line. The points for the aliphatic substituents are above the line and give an approximate linear line with a higher slope of 1.1 ($R^2 = 0.991$). The three aliphatic α -substituents give a similar line when the B3LYP/3-21+G* values are used (Fig. 6), with the point for Ph well below this line. This encourages the use of the RHF/3-21G* values. A similar plot for $\Delta G_{\text{eq}}^{\circ}$ in the gas phase vs. the calculated ΔE_{eq} values also gave a linear correlation for the four aromatic substituents with a slope of 1.04 ($R^2 = 0.993$) but the points for Mes and *t*-Bu were above the line, and a line drawn through them has a slope of 0.55 ($R^2 = 0.993$). The non-linearity for all the substituents is reminiscent of the behavior in hexane where the change in bulk of aliphatic and aromatic substituents causes an opposite change in K_{Enol} .^{5,6}

Geometry of and charges on the anions

The RHF/3-21G* calculated dihedral angles of the aryl groups with the double bond in both the neutral enols and their enolates are given in Table 3. Also given are the values for four enols and enolates calculated at the B3LYP/3-21G* and

Table 3 Calculated Ar–C=C dihedral angles (in degrees) in the enols **3** and the enolate ions **3⁻** at various levels: RHF/3-21G* (no parentheses), B3LYP/3-21G* (round parentheses), B3LYP/3-21+G* (square parentheses)

	R	β-Mes	β'-Mes	R	β-Mes	β'-Mes
<i>p</i> -MeC ₆ H ₄	28.7	57.1	59.4	25.4	52.9	52.0
C ₆ H ₅	29.4; 33.3^a	57.1; 62.4^a	59.5; 65.7^a	25.9	51.9	52.9
	(23.9); [29.1]	(56.1); [53.7]	(58.1); [58.7]	(20.0); [28.7]	(50.6); [50.1]	(48.8); [50.8]
<i>m</i> -ClC ₆ H ₄	28.5	57.4	59.4	24.6	52.3	52.3
<i>p</i> -CF ₃ C ₆ H ₄	28.5	57.4	59.5	25.5	52.5	53.2
Mes	55.6; 53.9^{a,b}	53.9; 53.9^{a,b}	61.5; 54.6^{a,b}	57.2	52.7	54.5
H ^d	—	52.3; 50.2^{a,c}	60.2; 56.7^{a,c}	—	50.1	50.9
	—	(48.9); [45.9]	(59.2); [59.4]	—	(49.0); [47.4]	(47.1); [49.5]
Me ^d	—	59.5; 55.7^a	59.4; 57.5^a	—	55.4	51.9
	—	(57.1); [55.9]	(58.9); [57.9]	—	(52.7); [51.7]	(47.7); [49.1]
<i>t</i> -Bu ^d	—	66.5; 63.7^a	59.3; 66.0^a	—	61.2	53.3
	—	(63.9); [62.8]	(58.5); [58.6]	—	(57.8); [57.8]	(48.2); [50.7]
SiMe ₃ ^d	—	62.9	58.5	—	59.6	50.8

^a Angles from X-ray diffraction are given in bold. ^b Average for two independent molecules. ^c Average for four independent molecules. ^d Previously calculated MM values (R, MM2(85),^{17b} MM2*^{17c}), H, β-Mes 48.4° β'-Mes 57.8°, β-Mes 50.7° β'-Mes 57.6°; Me, β-Mes 56.2° β'-Mes 56.2°, β-Mes 59.8° β'-Mes 56.5°; *t*-Bu, β-Mes 62.0° β'-Mes 55.8°, β-Mes 68.9° β'-Mes 57.2°; Me₃Si, no data available, β-Mes 67.8° β'-Mes 56.9°.

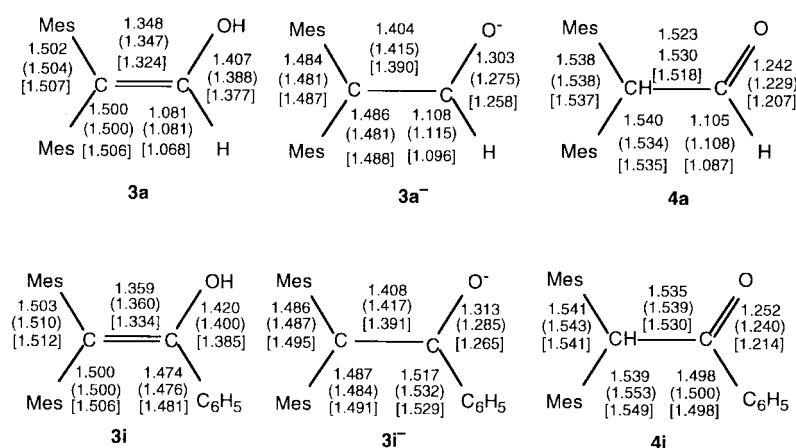


Fig. 7 Calculated B3LYP/3-21+G* (no parentheses), B3LYP/3-21G* (round parentheses) and RHF/3-21G* (square parentheses) bond lengths (in Å) in **3**, **3⁻** and **4** for α -H and α -Ph systems.

B3LYP/3-21+G* levels and by the MM2 method and X-ray diffraction values from the literature for the enols. The characteristic features for the enols are: (i) the B3LYP/3-21+G* values are always lower than the RHF/3-21G* values, by 6.4–3.4° (β-Mes) and 1.5–0.7° (β'-Mes) in the enols and 3.4–1.6° (β-Mes) and 2.8–1.4° (β'-Mes) in the enolates; (ii) a remarkable insensitivity of the angle for the β'-mesityl ring *cis* to the OH, the angle being 59.6 ± 0.5° at RHF/3-21G* and 59.1 ± 0.5° at the other levels; (iii) for the β-mesityl ring *trans* to the OH the angle ranges from 52.3° for α -H to 66.5° for α -*t*-Bu at RHF/3-21G* and from 48.9° to 63.9° at B3LYP/3-21+G*. For **3h–k** the angles for the α -Ar rings are nearly constant, being 28.8 ± 0.3°, but with a different angle of 55.6° for α -mesityl. These calculated values could be compared with the values determined by X-ray diffraction in solid **3a,b,e,g,i** and with the molecular mechanics calculated values for them and for **1f**. The X-ray diffraction angles for **3i⁻** are 4–6° (4–9°) higher than the RHF/3-21G* (B3LYP/3-21+G*) calculated ones whereas those for **3g¹⁶** are lower for ring β' and for ring α but are identical with those for ring β (Table 3).

For the aliphatic enols the calculated RHF/3-21G* angles are 2–3.5° higher than the X-ray values^{17a,b} for **3a** and **3b**, but lower for the β' ring and higher for the β ring of **3e**. At the B3LYP/3-21+G* level the calculated angles for **3a** are lower by 5–7° than the observed ones, are very similar for **3b** and higher by

0.5–3° for **3e**. The angles derived by *ab initio* methods are higher than the values determined by the MM2 (85) method^{17b} for **3a**, **3b** and **3e**, but the recent MM2* values^{17c} are in most cases (**3b**, **3e**, **3f**) higher than the *ab initio* derived values.^{17c}

It is interesting to compare the dihedral angles for the neutral enols **3** and their anions **3⁻**. The expectation is for as much planarization of the rings with the C=C–O⁻ moiety as possible in order to increase the extent of conjugation. However, the changes in the dihedral angles of the rings are not very large. At the B3LYP/3-21+G* level all the angles decrease on ionization by 8–12° for the β' ring and 3–5° for the β ring, except for a 1.5° increase for the β ring of **3a**. Changes of a similar magnitude are also found at the RHF/3-21G* level. The changes in all the three rings together cannot result in an increase in conjugation energy of more than 1–1.5 kcal mol⁻¹. We ascribe these small to medium changes to the rigidity of the systems that do not have much flexibility for rotation due to steric interactions between the three rings.

A comparison between the B3LYP/3-21+G* calculated bond lengths of the enol **3**, enolate **3⁻**, and “ketone” **4** of α -H and α -phenyl derivatives is shown in Fig. 7 and a similar comparison for the α -Me and α -*t*-Bu derivative is shown in Fig. S1 of the electronic supplementary information. In all cases, the ionization of **3** to **3⁻** results in an appreciable elongation of the C_α–C_β bond, a shortening of the Mes–C and C–O bonds, and

elongation of the C_α–R bond. Compared with **4** the three bonds to C_β of **3**[−] shrink and the C–O and C–R bonds elongate. The changes are similar for α-H, α-Me and α-*t*-Bu systems. These results are as expected when a charge is introduced into a 1-oxoallylic system. The elongation of the C–*t*-Bu bond in **3e**, **3e**[−] and **4e** is noteworthy, especially in **3e**[−] where the bond length is 1.585 Å.

The charge distributions at the respective atomic positions and groups as given by natural population analysis in the nine enolate ions are given in Fig. S2 of the electronic supplementary information. Atomic charges on hydrogens are summed into heavy atoms. With the caution required at the low level RHF/3-21G* level, the oxygen, C_β and its substituents are negatively charged, except that the β'-Mes in the α-Me₃Si anion **3f**[−] and C_α is always positive. The α-Me and α-*t*-Bu carry a negative charge whereas the electropositive α-Me₃Si is positively charged compared with the rest of the molecule. Consequently, C_α is the least positively polarized and is almost unchanged in the α-Me₃Si derivative. Ring β' is always more negative than ring β except for **3f**[−]; for the α-aryl-substituted enolates **3g**[−]–**3k**[−] the charge at C_α increases slightly with the increased electron-withdrawal by the aryl group, except for the α-mesityl group.

Conclusions

The pK_a^E, pK_a^K and the derived pK_{Enol} values for simple stable enol–ketone systems have been measured for the first time in the gas phase. The ΔG_{acid}^o values of the enols are an order of magnitude higher than in solution. The pK_a^E values in the gas phase are not linearly correlated with those in DMSO, suggesting the operation of additional effects, such as solvation and perhaps ion pairing in solution and a difference in the relative importance of polarizability in the two media. The pK_{Enol} values in the gas phase and in hexane are linearly correlated only for the Hammett series of α-aryl derivatives but not for other enols with bulky α-R's. Linear correlations were observed between ΔG_{acid}^o values and the *ab initio* calculated ΔE_{acid}^o values for the enols or the ketones. An interesting observation is the calculated relatively small to modest changes in the Ar–C=C dihedral angles on ionization, presumably due to the rigidity of the systems.

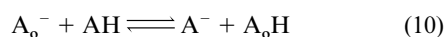
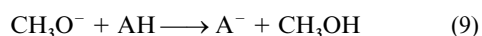
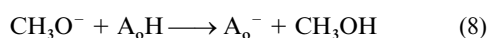
Experimental

Compounds

The enols and ketones were available from previous studies.^{5–8,11}

Gas-phase acidity measurements

The gas phase acidity measurements were performed on an Extrel FTMS 2001 Fourier transform mass spectrometer. Most of the experimental techniques used for the measurements of the equilibrium constants of the reversible proton-transfer reactions (2a)–(3b) are the same as in the literature.¹⁸ Only changes and additional procedures will be given here. Eqns. (7)–(10) describe the sequence of reactions which occurs in a typical



experiment. An experiment is initiated by a 5 ms pulse of a low-energy electron beam (0.3 to 0.5 eV) through the ICR cell. The electrons are captured by methyl nitrite at a partial pressure of 1.2×10^{-7} Torr and CH₃O[−] is produced. The acids AH and the

reference acid A_oH react rapidly with CH₃O[−] to yield M-1 negative ions. The partial pressure of the enols and ketones was maintained at less than 1.5×10^{-7} Torr because of their low volatility. The mass spectra and time plots were acquired and processed in an FT mode. The proton transfer equilibrium was achieved within 5 to 20 s of initiation of the reaction (depending on the pressure of neutrals), and the equilibrium constant *K* for eqn. (1) was evaluated using the expression $K = [\text{A}^-][\text{A}_o\text{H}]/[\text{A}_o^-][\text{AH}]$. The relative abundances of A[−] and A_o[−] ions were determined by the relative intensities of ICR mass spectral peaks when the equilibrium was attained. The pressures of the neutral reactants were measured by means of a Bayard–Alpert type ionization gauge with appropriate correction factors being applied to correct the gauge readings for the different ionization cross-sections of various compounds.¹⁹ Each experiment was performed at several ratios of the partial pressures and at different overall pressures. The arithmetic means of the values of *K* were used to calculate ΔG^o values at 323 K, the average uncertainty being ±0.2 kcal mol^{−1} in most of these cases. Each value was measured with two reference acids. The gas-phase acidity values for the reference compounds were taken from the literature.¹⁵ All of the compounds investigated in this study are low volatility solids. The solid sample direct-inlet system and the ICR chamber were kept at 100 °C. Each sample was sublimed under a vacuum line to remove entrapped volatile impurities.

The conjugate base of **6** as well as the reference acids were generated by a reaction with methoxide ions and its amount reached a maximum within several hundred ms. When the anion **5**[−] was ejected from the ICR cell by means of the SWIFT technique, its formation by a proton transfer between the neutral **6** and the conjugate anion of the reference acid, was quite slow. After even 50 seconds the relative abundance ratio of **5**[−] to the reference anion was smaller than that observed under no ion-ejection conditions, indicating that an equilibrium was not achieved. At this long reaction time the concentration of the reference anion significantly decreased to form the hydrogen bonded dimer [ROHR][−]. The acidity of **6** in Fig. 1 was obtained from the initial abundance of the ions generated by the reaction with MeO[−]. It therefore seems that the value is that of the kinetic rather than the thermodynamic acidity.

Calculations

All *ab initio* LCAO-MO calculations were performed using the GAUSSIAN94 program.²⁰ The closed-shell restricted Hartree–Fock calculation with an STO 3-21G* basis set was applied to find a stationary point on the potential energy surface. The Hybrid Density Functional Theory method used the B3LYP Functional.²¹

References

- For reviews on enols see, *The Chemistry of Enols*, ed. Z. Rappoport, John Wiley, Chichester, 1990.
- J. Toullec, in *The Chemistry of Enols*, ed. Z. Rappoport, John Wiley, Chichester, 1990, ch. 6, p. 323.
- J. R. Keeffe and A. J. Kresge, in *The Chemistry of Enols*, ed. Z. Rappoport, John Wiley, Chichester, 1990, ch. 7, p. 399.
- (a) H. Hart, *Chem. Rev.*, 1979, **79**, 515; (b) H. Hart, Z. Rappoport and S. E. Biali, in *The Chemistry of Enols*, ed. Z. Rappoport, John Wiley, Chichester, 1990, ch. 8, p. 481; (c) Z. Rappoport and S. E. Biali, *Acc. Chem. Res.*, 1988, **21**, 442.
- D. A. Nugiel and Z. Rappoport, *J. Am. Chem. Soc.*, 1985, **107**, 3669.
- S. E. Biali and Z. Rappoport, *J. Am. Chem. Soc.*, 1985, **107**, 1007.
- E. B. Nadler and Z. Rappoport, *J. Am. Chem. Soc.*, 1987, **109**, 2112.
- E. B. Nadler, Z. Rappoport, D. Arad and Y. Apeloig, *J. Am. Chem. Soc.*, 1987, **109**, 7873.
- F. G. Bordwell, S. Zhang, I. Eventova and Z. Rappoport, *J. Org. Chem.*, 1997, **62**, 5371.
- M. Röck and M. Schmittel, *J. Chem. Soc., Chem. Commun.*, 1993, 1739.

- 11 E. B. Nadler and Z. Rappoport, *J. Org. Chem.*, 1990, **55**, 2673.
- 12 Preliminary communication: Z. Rappoport, I. Eventova, M. Mishima, Mustanir, S. Zhang and F. G. Bordwell, ICPOC-14 Post Conference Symposium on Recent Advances in Organic Reaction Mechanisms, Puerto Iguazu, Argentina, August 23–24, 1998, Abstr. p. 13.
- 13 Z. Rappoport, D. A. Nugiel and S. E. Biali, *J. Org. Chem.*, 1988, **53**, 4814; E. B. Nadler and Z. Rappoport, *J. Am. Chem. Soc.*, 1989, **111**, 213.
- 14 R. W. Taft and R. D. Topsom, *Prog. Phys. Org. Chem.*, 1987, **16**, 1.
- 15 S. E. Lias, J. E. Bartmess, J. F. Liebman, J. L. Holmes, R. D. Levin and G. W. Mallard, *J. Phys. Chem. Ref. Data*, 1988, **17**, Suppl. 1.
- 16 M. Kaftory, S. E. Biali and Z. Rappoport, *J. Am. Chem. Soc.*, 1985, **107**, 1701.
- 17 (a) M. Kaftory, D. A. Nugiel, S. E. Biali and Z. Rappoport, *J. Am. Chem. Soc.*, 1989, **111**, 8181; (b) S. E. Biali, D. A. Nugiel and Z. Rappoport, *J. Am. Chem. Soc.*, 1989, **111**, 846; (c) J. Frey, E. Schottland, Z. Rappoport, D. Bravo-Zhivotovskii, M. Nakash, M. Botoshansky, M. Kaftory and Y. Apeloig, *J. Chem. Soc., Perkin Trans. 2*, 1994, 2555.
- 18 M. Fujio, R. T. McIver, Jr. and R. W. Taft, *J. Am. Chem. Soc.*, 1981, **103**, 4017.
- 19 (a) J. E. Bartmess and R. M. Georgiadis, *Vacuum*, 1983, **3**, 149; (b) K. J. Miller, *J. Am. Chem. Soc.*, 1990, **112**, 8533.
- 20 GAUSSIAN94, Revision C.2, M. J. Frisch, G. W. Trucks, H. B. Schlegel, P. M. W. Gill, B. G. Johnson, M. A. Robb, J. R. Cheeseman, T. Keith, G. A. Petersson, J. A. Montgomery, K. Raghavachari, M. A. Al-Laham, V. G. Zakrzewski, J. V. Ortiz, J. B. Foresman, J. Cioslowski, B. B. Stefanov, A. Nanayakkara, M. Challacombe, C. Y. Peng, P. Y. Ayala, W. Chen, M. W. Wong, J. L. Andres, E. S. Replogle, R. Gomperts, R. L. Martin, D. J. Fox, J. S. Binkley, D. J. Defrees, J. Baker, J. P. Stewart, M. Head-Gordon, C. Gonzalez and J. A. Pople, Gaussian, Inc., Pittsburgh, PA, 1995.
- 21 (a) A. D. Becke, *J. Chem. Phys.*, 1993, **98**, 1372, 5648; *Phys. Rev. A*, 1988, **38**, 3098; (b) C. Lee, W. Yang and R. G. Paar, *Phys. Rev. B*, 1988, **37**, 785.